Journal of Physics: Conference Series **3177** (2026) 012068 doi:10.1088/1742-6596/3177/1/012068

Virgo h(t) reconstruction for O4 and O5

F. Aubin[1], C. Grimaud[2], B. Mours[1], T. Pradier[1], L. Rolland[2], M. Seglar-Arroyo[3], A. Syx[1], H. Van Haevermaet[4], P. Van Hove[1], D. Verkindt[2]

[1]Université de Strasbourg, CNRS, IPHC UMR 7178, F-67000 Strasbourg, France

[2]Laboratoire d'Annecy de Physique des Particules (LAPP), Univ. Grenoble Alpes, Université Savoie Mont Blanc, CNRS/IN2P3, F-74941 Annecy, France

[3]Institut de Fısica d'Altes Energies (IFAE), Barcelona Institute of Science and Technology, and ICREA, E-08193 Barcelona, Spain

[4]Universiteit Antwerpen, Prinsstraat 13, 2000 Antwerpen, Belgium

E-mail: verkindt@lapp.in2p3.fr

Abstract. The precise online reconstruction of the Virgo detector strain $h(t)$ induced by gravitational waves is the main detector output used for astrophysical observations. Its latency is critical for the low-latency alerts generation. Since the start of the O4 run, a new version of the Virgo $h(t)$ reconstruction process in the frequency domain is used and provides an unbiased and noise-mitigated $h(t)$ with frequency-dependent one sigma uncertainties around 2% on modulus and 30 mrad on phase, and with a latency below 10 seconds. In parallel, a time domain $h(t)$ reconstruction is under study to provide at least the same features and performance while improving the latency down to about one second. The principle, main features and results of those two types of $h(t)$ reconstruction, developed within the Virgo calibration team, are presented here.

1 Introduction

The Advanced Virgo interferometer [1] is the European detector participating since 2017 to the gravitational wave astronomy. Since the first detection of gravitational waves from a binary black hole [2] or a binary neutron star [3], the LIGO and Virgo interferometers network has provided hundreds of online detected events during the observing runs O2, O3 and O4 [4][5]. Each of those events is the result of online data analysis pipelines taking as input a gravitational wave strain $h(t)$ provided by each detector.

This strain is not directly the dark fringe signal provided by the photodiodes at the output of the interferometer, because the longitudinal controls of the intereferometer, especially the Differential Arm length control (DARM), get parts of the strain signal. The Virgo $h(t)$ is reconstructed by an online process named Hrec which takes as inputs the dark fringe signal and the longitudinal control signals acting on the interferometer mirrors.

The principle of $h(t)$ reconstruction used in O4 and described in the next section is shown in Figure 1, which includes the additional steps of unbiasing and noise subtraction.

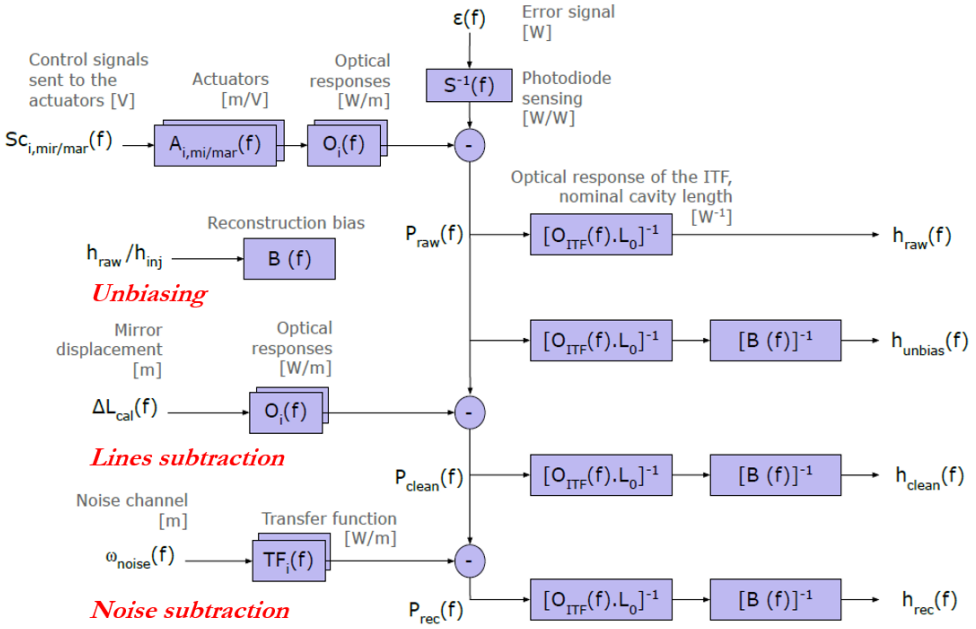

Figure 1: (a) Schematic of the Virgo h(t) reconstruction in O4 that produce the h_raw values and of the steps added to the h(t) reconstruction (unbiasing and noise subtraction)

2 Low-latency h(t) reconstruction for O4

The Hrec process [6] works currently in the frequency domain and uses FFTs of the dark fringe signal and of the control signals computed over a time window of 8 seconds. This implies for this process a minimal latency of 8 seconds, but provides a quite easy signal processing (simple way to apply actuators or optical response models, simpler way to apply high-pass filtering or resampling) with a good frequency resolution of 0.125 Hz.

For each interferometer's mirror, an actuator's model is available thanks to the calibration injections and measurements done every week [7], which take as reference the signal provided by the Photon Calibrator [8][9][10]. Using this actuator's model and the approximated single pole optical response model (see figure 2), Hrec can build, for each mirror control signal, the contribution to be added to the dark fringe signal in order to obtain the light power variations of the dark fringe due to the interferometer's arm length variations. In addition, Hrec can adjust periodically the optical response model parameters (pole frequency and optical gain), thanks to two sinusoidal signals injected permanently on each mirror actuator. Finally, an averaged inverse optical response is used to obtain the length variation at the origin of the light power variation reconstructed by Hrec. The reconstructed $h(t)$ is this length variation divided by the interferometer arm length.

With respect to the Hrec process used in O3, several changes have been made for O4. The first one is the possibility to use a different optical response model for each mirror. This allows to use a specific optical response for Power Recycling (PR) and Signal Recycling (SR) mirrors. Second main improvement is the possibility to unbias online the $h(t)$ values, thus allowing to provide to online analyses an $h(t)$ with a frequency-dependent residual bias close to zero. This unbiasing operation is done thanks to weekly measurements done on this bias for a set of 27 frequencies [11].

In addition, during O4, Hrec computed the bias values (called hrec/hinj) for a set of permanent lines injected on North End (NE) mirror and West End (WE) mirror actuators. If the modulus of hrec/hinj is around 1 and the phase around 0, its means that $h(t)$ was reconstructed properly with respect to the hinj values computed from the injections.

3 Plans and first results of low-latency h(t) reconstruction for O5

During O4, because of the interferometer's optical configuration, with SR mirror misaligned in order to deal with Virgo marginally stable cavities, the longitudinal control of SR and PR were not taken into

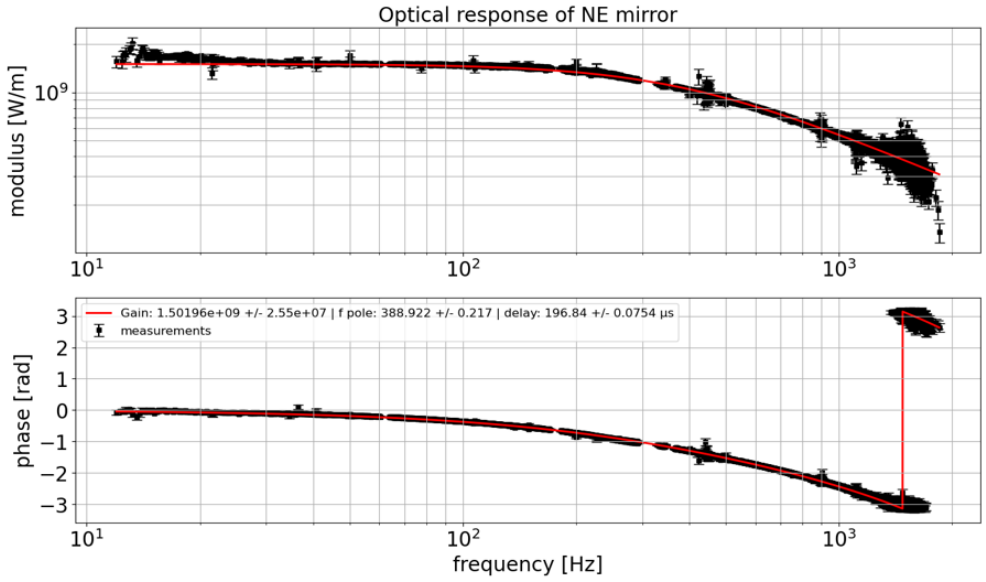

Figure 2: Optical response measurement and the single pole fit done to obtain the optical response model.

account for $h(t)$ reconstruction. For next observing runs, Virgo will have stable cavities. Thus, a first improvement for $h(t)$ reconstruction will be to deal with the optical response of stable cavities and to take PR and SR into account. In addition, we plan to reduce the residual bias of the $h(t)$ reconstruction by better modeling the optical response and better adjusting it through the monitoring of its short time-scale fluctuations.

This will be done either by continuing to use the mirrors control signals to do the h(t) reconstruction (what we call the "mirror referential"), as we did in O3 and O4, or by using directly the knowledge of the DARM control closed loop transfer function to reconstruct $h(t)$ from the DARM signal (what we call the "DARM referential"), following the way LIGO detectors do the h(t) reconstruction.

A second improvement is to decouple the $h(t)$ reconstruction from the linear noise subtraction so that the code associated to the noise subtraction can be managed offline and online independently of the $h(t)$ reconstruction package.

One main final improvement is the reduction of the latency of the online $h(t)$ reconstruction down to about one second, so that this latency becomes negligible with respect to the full latency of the online data analysis chain down to the alerts. This is one of the steps needed for the early-warning alerts sent before the binary neutron star mergers.

3.1 Reconstruction in the time domain with IIR filters: HrecAcl

The latency reduction can be obtained in the time domain by using, within the Virgo framework used for real-time controls, a set of Infinite Impulse Response (IIR) filters to apply the actuators models and the optical response models. Those filters need to use additional delays in order to synchronize them and to keep the causality of the process. Such delays are then taken into account when providing $h(t)$.

The detail of this processing is shown in Figure 3. The first part contains the main steps of the $h(t)$ reconstruction and has a full latency of about 300 μs. In a second step, in order to apply the high-pass filter which reduces the dynamic of $h(t)$ and also to provide with low computing consumption an $h(t)$ resampled at 16384 Hz, the $h(t)$ is submitted to a FFT made over a time window of 1 second. This increases the total latency of HrecAcl to about 1 second.

Figure 4 shows the transfer function and the coherence between $h(t)$ of Hrec and $h(t)$ of HrecAcl. It must be noted that, in HrecAcl, the parameters of optical response model were forced to be the same as those of Hrec, as the periodic update of the optical response model was not yet available in the time domain framework. This may explain the good transfer function between HrecAcl and Hrec, with a modulus around 1 and a phase around 0. The HrecAcl method has the advantage to reconstruct $h(t)$ with a very low latency and to use a limited CPU consumption within an already existing real-time

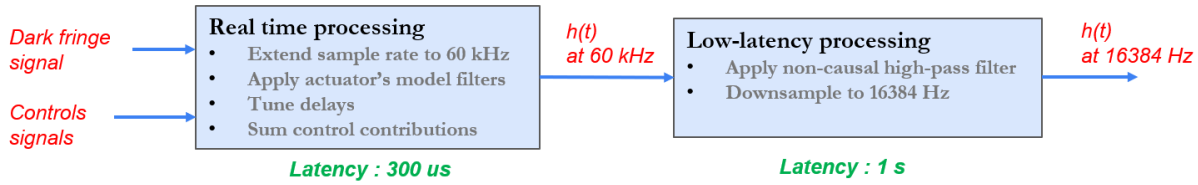

Figure 3: Scheme of the HrecAcl h(t) reconstruction in the time domain.

framework. It has the drawback to be less flexible than the use of the frequency domain and to be attached to the use of the existing real-time framework (so not running on an independent machine).

3.2 Reconstruction in the frequency domain with zero-padding: HrecDFT

The latency reduction has been explored also in the frequency domain, using input data chunks of one second zero-padded to a well-chosen number of seconds before computing the FFTs. In addition, a high-pass filter is needed to reduce the large dynamic of the reconstructed $h(t)$ and to remove the noise that may be associated with it. Using in HrecDFT a zero-padding done over 1 sec before and 1 sec after the chunk of data, we got $h(t)$ values that we compared to the O4 data provided by Hrec. It shows some lack of coherence below 100 Hz, maybe due to the optical response adjustment not yet implemented in HrecDFT. This is still under investigation. The HrecDFT method has the advantage to be more flexible, especially if we want to add other processings like unbiasing or noise mitigation and to run on a dedicated machine separate from the real-time framework. It has the drawback of a larger CPU consumption and a larger latency (4 seconds of data are processed in 1 second if we want to reach a latency of 3 seconds).

All this work on HrecDFT and HrecAcl is preliminary and has been done mainly by Brian Huchon, in his Master2 internship [12].

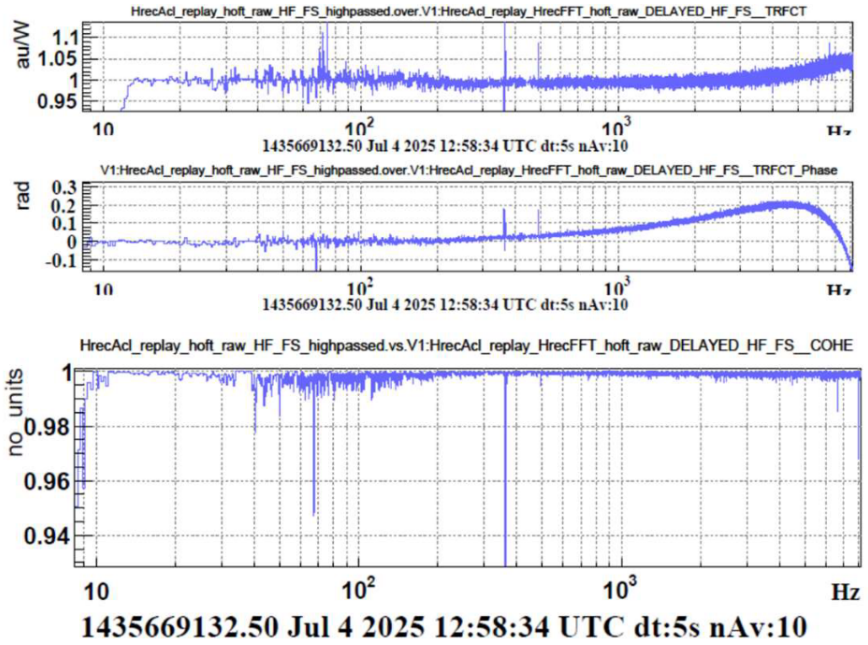

Figure 4: Transfert function and coherence between h(t) from Hrec and h(t) from HrecAcl.

4 Acknowledgments
The authors gratefully acknowledge the Italian Istituto Nazionale di Fisica Nucleare (INFN), the French Centre National de la Recherche Scientifique (CNRS) and the Netherlands Organization for Scientific Research (NWO), for the construction and operation of the Virgo detector and the creation and support of the EGO consortium. The authors also gratefully acknowledge research support from these agencies as well as by the Spanish Agencia Estatal de Investigación, the Consellera d'Innovació, Universitats, Ciència i Societat Digital de la Generalitat Valenciana and the CERCA Programme Generalitat de Catalunya, Spain, the National Science Centre of Poland and the European Union – European Regional Development Fund; Foundation for Polish Science (FNP), the Hungarian Scientific Research Fund (OTKA), the French Lyon Institute of Origins (LIO), the Belgian Fonds de la Recherche Scientifique (FRS-FNRS), Actions de Recherche Concertées (ARC) and Fonds Wetenschappelijk Onderzoek – Vlaanderen (FWO), Belgium, the European Commission. The authors gratefully acknowledges support from the French Agence Nationale de la Recherche for the project ACALCO (ANR-21-CE31- 0024). The authors gratefully acknowledge the support of the NSF, STFC, INFN, CNRS and Nikhef for provision of computational resources.

References
[1] F. Acernese et al. Advanced Virgo: a second-generation interferometric gravitational wave detector. *Class. Quant. Grav.*, 32(2):024001, 2015.

[2] B. P. Abbott et al. GW170814: A Three-Detector Observation of Gravitational Waves from a Binary Black Hole Coalescence. *Phys. Rev. Lett.*, 119:141101, Oct 2017.

[3] B. P. Abbott et al. GW170817: Observation of Gravitational Waves from a Binary Neutron Star Inspiral. *Phys. Rev. Lett.*, 119:161101, Oct 2017.

[4] R. Abbott et al. GWTC-3: Compact Binary Coalescences Observed by LIGO and Virgo during the Second Part of the Third Observing Run. *Phys. Rev. X*, 13:041039, Dec 2023.

[5] A. G. Abac et al. GWTC-4.0: Updating the Gravitational-Wave Transient Catalog with Observations from the First Part of the Fourth LIGO-Virgo-KAGRA Observing Run, https://arxiv.org/abs/2508.18082. 2025.

[6] L. Rolland M. Seglar-Arroyo D.Verkindt D. Estevez, B. Mours. Hrec package documentation. *Virgo note*, (VIR-0590B-20), 2025.

[7] F. Acernese et al. Calibration of Advanced Virgo and reconstruction of the detector strain h(t) during the observing run O3. *Class. Quant. Grav.*, 39(4):045006, 2022.

[8] A. Masserot L. Rolland-M. Seglar-Arroyo D. Estevez, P. Lagabbe and D. Verkindt. The Advanced Virgo Photon Calibrators. *Class. Quant. Grav.*, 38:075007, 2021.

[9] P. Lagabbe. *Improving the Advanced Virgo+ calibration with the photon calibrator for the 04 run.* PhD thesis, Universite Savoie Mont-Blanc, 2023.

[10] C. Grimaud. *Virgo interferometer calibration and h(t) detector strain reconstruction uncertainty computation during the O4 observing run.* PhD thesis, Universite Savoie Mont-Blanc, 2025.

[11] C. Grimaud. From the Virgo interferometer calibration to the bias and uncertainty of the h(t) detector strain during the o4 run. *in these proceedings.*

[12] B. Huchon. M2 internship report: Development of two low-latency reconstruction methods of the gravitational wave strain signal h(t) for Virgo. *Virgo note*, (VIR-0834A-25), 2025.